Impact of Oxygen Enrichment and CO2–H2O Dilution on Stability and Pollutant Emissions of Non-Premixed Swirling Turbulent Flames

Impact of Oxygen Enrichment and CO2–H2O Dilution on Stability and Pollutant Emissions of Non-Premixed Swirling Turbulent Flames

Impact of Oxygen Enrichment and CO_2-H_2O Dilution on Stability and Pollutant Emissions of Non-Premixed Swirling Turbulent Flames

Toufik Boushaki[1,2,*], Hajar Zaidaoui[1], Sawssen Chakchak[1], Ahlem Ghabi[1], Ahmed I. Abd El-Rahman[2,3], Ahmed. F. Ghoniem[2]

[1]ICARE CNRS - University of Orleans, 1C. Avenue de la Recherche Scientifique, Orleans, France

[2]Reacting Gas Dynamics Laboratory, Department of Mechanical Engineering, Massachusetts Institute of Technology, 77 Massachusetts Avenue, Cambridge, MA 02139, United States

[3]Department of Mechanical Power Engineering, Cairo University, Giza 12613, Egypt

*Corresponding author's contact information:

Dr. Toufik BOUSHAKI,

ICARE, CNRS

1C, Avenue de la Recherche Scientifique, 45071 Orléans, France

Email address: toufik.boushaki@cnrs-orleans.fr

Abstract

The aim of this work is to investigate the effect of exhaust gas recirculation (EGR: water vapor and CO_2), with and without O_2 enrichment, on non-premixed turbulent flames stabilized on a swirl burner. The motivation includes CO_2 capture applications using O_2 and CO_2, combustion of biogas that containing CO_2 and the use of EGR or H_2O in certain industrial applications to reduce pollutant emissions. Experiments were carried out on a coaxial swirl burner placed in a combustion chamber of 25 kW nominal power. The oxidant (air-O_2, +H_2O, +CO_2) is introduced in the annular part though a swirler. The fuel (CH_4) is fed though the central tube and injected radially at the exit section. The study focuses on laminar burning velocity, pollutant emissions, flame stability, and flow fields measurements with different fractions of O_2, H_2O and CO_2 in the mixture. The fraction of diluents is varied from 0 to 20%, O_2 concentration from 21 to 25% (in vol.) and the swirl number from 0.8 to 1.4. Different measurements are recorded: OH* chemiluminescence to locate the flame front, Stereo-PIV to analyze the flow field, pollutant emissions analysis (NOx and CO) and temperatures in the combustion chamber. Results show that dilution significantly influences flame characteristics. Dilution increases the lift-off height and reduces flame stability especially with high fractions (16-20%), whereas O_2 enrichment decreases lift-off height and enhances flame stability. The increase dilution reduces NOx and increases CO emissions. Stereo-PIV measurements reveals the turbulent coherent structure of the swirling flow as well as the effect of dilution on the corresponding axial and tangential velocities. The effect of dilution on the underlying laminar burning velocity were determined by 1D calculation using COSILAB with GRI3.0 mechanism.

Keywords Flame stability - Swirling flame - Oxygen enrichment - Pollutant emissions - CO_2-H_2O dilution

3

Introduction

Regulations of harmful exhaust emissions and fuel economy are becoming more stringent, and hence current measures of combustion performance are more focused on pollutant emissions and combustion efficiency. Dilution of combustion by EGR (Exhaust Gas Recirculation) gases is considered an effective technique to reduce pollutant emissions, especially NOx. Such technique is commonly used in internal combustion engines (Abd-Alla 2002, Sher 1998, Zheng et al. 2004). Several research studies investigated EGR in other combustion systems (Yu et al. 2013, Shimokuri et al. 2015, Granados et al. 2014, Minamoto et al. 2013, Jangi et al. 2013, Yu al. 2015). Shimokuri et al. (2015) investigated NOx emission in oxy-fuel premixed combustion of $CH_4/O_2/CO_2$ mixture using a tubular flame burner with Flue Gas Recirculation (FGR). They observed that NOx concentrations depend strongly on the oxygen contents and the equivalence ratio under non-preheating conditions, while the NOx concentration approached the same values for all O_2 concentration conditions with preheating. Yu et al. (2015) studied NOx emission in CH_4/air non-premixed swirling flames with EGR using Air-EGR (EGR injected with air) and Fuel-EGR (EGR injected with fuel). They reported that NOx concentration decreases with EGR due to a drop in flame temperature in both cases. They noticed also that the Fuel-EGR method exhibited better results than the Air-EGR on pollutant emissions at the same EGR ratios. Gu et al. (2006) demonstrated significant impacts of water vapor on non-premixed flame stability and recirculation zone structure. Regarding the case of CH_4-air and natural gas-air flames, LeCong and Dagaut (2009) showed that the addition of H_2O led to lower flame speed, lower flame temperature, as well as lower NOx. Boushaki et al. (2012) experimentally showed the reduction in the laminar burning velocity and flame temperature with steam addition of premixed flames, both attributed to thermal effect. Other works, with focus on diffusion flames, showed that CO2 dilution causes reductions in flame temperature and thermal NO (Jeong et al. (2007). Branco et al. (2016) experimental study on turbulent

4

diffusion flames showed that CO_2 addition to forces the reaction to proceed further downstream, lowers the intensity of OH and suppresses NO formation. Temperature reduction plays a very important role in the durability of burners. Dilution by CO_2, H_2O or using EGR may possibly yield severe flame instabilities, and even blow-outs if the diluents concentrations are significantly high. Oxygen enrichment at small fractions avoids these instabilities (Baukal 2013). An experimental study performed by Wu et al. (2010) on natural gas non-premixed flames indicated an increase of 53.6% in the heating rate and a reduction of 26.1% in the fuel consumption, as the oxygen concentration was raised from 20 to 30%, in the heating and furnace-temperature fixing tests, respectively. They also noted that the greater the oxygen concentrations the higher the flame temperature; and thus, the more serious the NO_x emission. Qiu et al. (2009) showed that an oxygen concentration of 28% offers about 22–28% potential natural gas savings for the gas-fired radiant burners because of the increased flame temperature that is associated with the imposed O_2 enrichment. For two types of porous ceramic premixed burners, the authors mentioned that the radiation output and, the consequent radiant efficiency increase markedly with the oxygen concentration in the combustion air. Baukal and Gebhart (1998) showed that the thermal efficiency (heat recovered/heat of combustion) more than doubled as the oxygen concentration was increased from 30 to 100 %. Boushaki et al. (2017) reported that oxygen enrichment in co-axial non-premixed burner is clearly advantageous for CO reduction and CO_2 augmentation in post-combustion CO_2 capture process.

This paper investigates the effects of EGR dilution and O_2 enrichment on a turbulent non-premixed swirling flame. O_2 enrichment is applied to control both flame stability and pollutant emissions. Swirling flows are extensively used to enhance mixing and improve flame stability via the formation of a central recirculation zone (CRZ) (Yuasa 1986, Merlo 2013, Mansouri and Boushaki 2018, Mansour et al. 2008), as well as the outer recirculation zones (ORZ) (Taamallah et al. 2017). The present paper focuses on the effect of EGR/O_2 on pollutant

5

emissions and flame stability using OH* chemiluminescence and stereo-PIV diagnostic in reacting conditions. In particular, the significance of this work lies behind the chosen burner configuration, the revealed strong dependence of the pollutant emissions and flame stability on the oxygen enrichment and CO_2/H_2O dilution, and the quantification of the different parameter's effects. The present burner consists of a coaxial configuration which contains a swirler, a radial injection of fuel via small holes, a confined turbulent flame, a non-premixed combustion. Although complicated, such configuration represents a practical burner, application of which has not been reported before. The oxygen enrichment (21 to 35%) and the dilution in CO_2-H_2O (0-20%) for EGR simulation are the main parameters under investigation in this work. Furthermore, the influence of two other important parameters is also examined: the swirl number that represent the geometric parameter, and the equivalence ratio that describes the chemical parameter. The quantification of the effects of these parameters on the pollutant emissions (CO and NOx), the lift off heights, the flame lengths and flow fields are reported in this paper.

Experimental setup

Combustion system

The present experimental setup includes a combustor with a swirl burner, heating system for steam production, gas analyzers and measurement techniques. The combustor is a parallelepiped chamber, as shown in Fig. 1, with a 500 mm square cross section and 1000 mm height equipped with six quartz or metallic window on each side, allowing large optical access to the flame region. At the top of the chamber, there is a converging section within 200 mm height to avoid ambient air entrainment through the combustor outlet. The flue gases exit to the atmosphere at ambient pressure. The walls of the chamber are cooled by internal water circulation, as shown in Fig. 1.

6

The swirl burner, shown in Fig. 2 is placed at the bottom center of the combustion chamber to maintain uniform axial and azimuthal developments of the flame. Notice that the burner outlet immerses of 3 cm the bottom plane of the combustion chamber. CH_4 is supplied radially by the central tube injector (D_i = 12 mm and D_e=15 mm) with eight holes of 3 mm inside diameter. Air, O_2, CO_2 and water vapor are mixed and injected through the coaxial tube (D_i = 15 mm and D_e=38 mm) which contains the swirler. A Bronkhorst CEM (controlled evaporation and mixing) system is used to generate and adjust water vapor flowrate, as shown on the right of Fig. 1. It includes a CORI-FLOW liquid flowmeter, a mass flowmeter for the carrier gas (air) and a temperature-controlled mixing/evaporation chamber. Note that during the dilution, the burner, mixer, seeder and gas lines are heated to avoid steam condensation before combustion and ensure an average temperature of 383 K at the burner exit. Swirling motion is produced by an eight-bladed swirler that is placed in the coaxial tube 50-mm away from the burner exit. The swirl number is defined as the ratio of the angular momentum flux G_Θ to the product of axial momentum flux G_Z times a characteristic length that typically refers to the radial dimension R as follows:

$$S_n = \frac{G_\Theta}{R\, G_z} \qquad (1)$$

The geometrical swirl number Sn for the present configuration can further expanded to (Beér and Chigier 1972, Gupta et al. 1984):

$$S_n = \frac{1}{1-\psi} \cdot \left(\frac{1}{2}\right) \cdot \frac{1-(R_h/R)^4}{1-(R_h/R)^2}\, tan\, \alpha_0 \qquad (2)$$

where α_0 is the vane angle, ψ is the blockage factor and R and R_h correspond to both nozzle and vane pack hub radii, respectively (Gupta et al. 1984). For instance, a Sn=1.4 corresponds to: R=17.5 mm, Rh=8.8 mm, α_0=60° and ψ=0.23. The blocking factor (ψ) depends on the thickness and the number of blade (see Chakchack and al. 2023).

7

The oxygen concentration in the oxidizer (Ω) is the ratio of oxygen flow rate to the total flow rate expressed as:

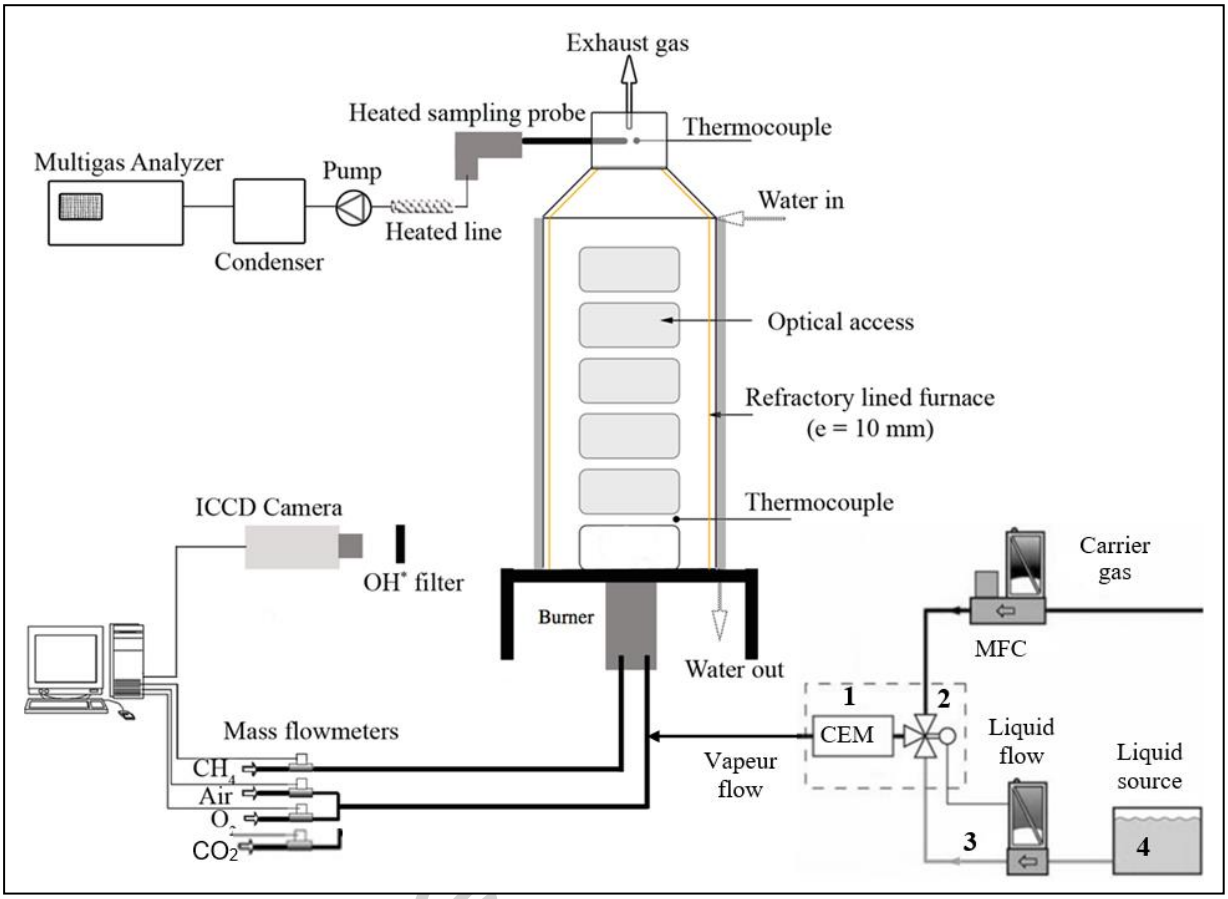

$$\Omega = \frac{Q_{O2}}{Q_{O2} + Q_{N2}} \qquad (3)$$

Fig. 1 Schematic diagram of the combustion system (chamber, chemiluminescence technique, gas supply system, gas analyzer, CEM "*Controlled Evaporation Mixing*" system).

8

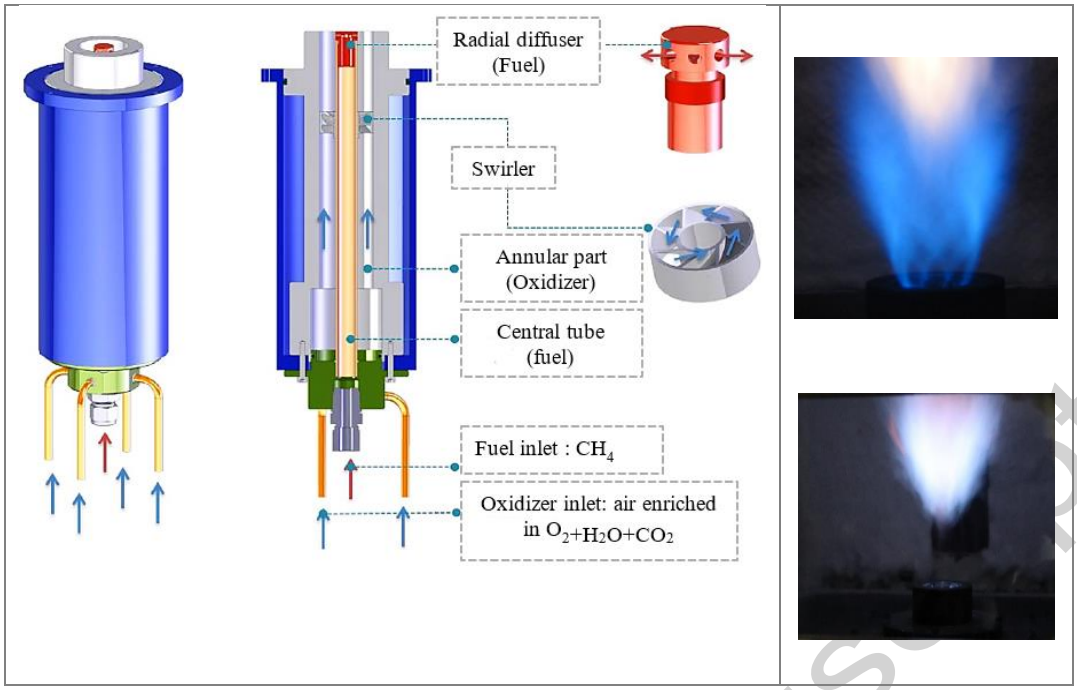

Fig. 2 Schematic of the coaxial swirl burner and an example of flames from the swirl burner

The CO_2, H_2O and EGR concentration (only relative to air flow rate) in the oxidizer is written as:

$$\%\ vol\ CO_2 = \frac{Q_{CO_2}}{Q_{air}}\ ,\quad \%\ vol\ H_2O = \frac{Q_{H_2O}}{Q_{air}},\quad \%\ vol\ EGR = \frac{Q_{H_2O} + Q_{CO_2}}{Q_{air}} \tag{4}$$

In the present work, the global equivalence ratio (at the injection point of fuel and oxidizer) is fixed to 0.8, the swirl number ranges from 0.8 to 1.4, the oxygen enrichment varies from 21 vol % to 30 vol %, and CO_2 and H_2O contents range from 0 vol % to 20 vol %. For instance, at without dilution and O_2 enrichment, at Φ=0.8, the corresponding flame power is 7.5 kW with 150l/min of air flow rate, 12.6 l/min of CH_4 flow rate, and Reynolds number of 4514. Since the oxidizer (air + diluent) flow rate remains constant, when 20% of CO_2 is injected, the air flow rate is 125 l/min, the CO_2 flow rate is 25 l/min, and corresponding flame power is 6.3 kW.

Measurement methods

9

Exhaust emissions, including CO, CO_2, O_2, and NO_X are measured using a Horiba PG250 multi-gas analyzer (accuracy of ±1% of full scale). Only CO and NO_X measurements are reported in this paper. The measurement uncertainties were estimates around 3%, including 1% of apparatus errors, 1% of measurement fluctuations and 1% of error users. Thermocouples are located along the combustion chamber for temperatures measurements of flue gases and chamber walls. For the uncertainty, two errors were taken into account, random and systematic. The random error is induced by the reading values and determined by the average value and standard deviation. It was estimated at 1% of the measured value. The systematic error is produced mostly by radiation and conduction of the thermocouple and estimated at around 0.5%. The flame shape, flame spatial position including lift-off heights and flame lengths are examined using chemiluminescence of OH*. The OH* chemiluminescence signal remains a good tracer of the reaction zone for high-temperature flames operating close to stoichiometry (Docquier and Candel 2002). The exposition time was set at 40 ms. The measurement field gave a real area of 112x112 mm² with 9.2 pixels/mm as a spatial resolution. The imaging acquisition was done on 300 instantaneous images to enable statistical calculations of parameters (converged average value and standard deviation) during the image processing. The image processing was performed using MATLAB code tailored to the types and sizes of images. The MATLAB program eases flame contour detection, enabling the determination of flame heights, flame lengths, and their respective standard deviations. The different sources of uncertainties in the measurements of flame heights and lengths are summarized in Table 1.

Table 1. Evaluation of the H_f and L_f measurements uncertainties.

Uncertainties source	**Estimate**
Conversion factor mm/pixel	± 0.8 %
Threshold value	± 3.5 %

10

Burner position	± 1 %
Total uncertainty	± 3.6 %

Both Chemiluminescence and gas analysis techniques are fully described by Zaidaoui et al. (2017).

Flow field measurements are performed using Stereoscopic Particle Image Velocimetry (Stereo-PIV) measurements. The flow is seeded with micro-metric ZrO_2 particles. Particles are injected in the coaxial tube. The SPIV system features a 2 x 130 mJ Nd:YAG laser double pulse (Quantel CFR200) at 532 nm operated at 10Hz and two 2048 x 2048 pixels CCD cameras from JAI (RM-4200CL, 12bits). Each of the two cameras mounted on Scheimpflug adapters is oriented on the corresponding side of the laser sheet. The cameras are equipped with two Carl Zeiss Milvus lenses (Makro-Planar T x 100mm f/2 ZF.2) and two interference filters to help reduce the flame signal on the second PIV image that is more exposed to the light and to collect only the diffusion Mie of seeded particles. Measurements are done in a longitudinal light sheet crossing the burner axis. The light sheet of 100x80 mm in dimensions has a thickness of 1mm to minimize out-of-sheet particles displacements of the swirling flow between the double laser pulses. Five hundred image pairs separated by 30 µs are recorded for each case to ensure reasonable statistical convergence of the mean and the RMS (root-mean-square) components of the velocity fields. The DynamicStudio by Dantec Dynamics is used to compute the velocity fields. The S-PIV calculation interrogation window size was set at 32×32 pixels which means 1.57×1.57 mm² in real size (1 pixel =0.049 mm). Velocity values and vector fields were calculated using the cross-correlation algorithm. With a maximum particle movement of 8 pixels, this induces to less than 5% uncertainty in the final velocity measurement.

11

Results and Discussions

Behavior and stability of flame

To evaluate the effect of dilution on the laminar burning velocity, 1D calculations of CH_4-air, CH_4-air-H_2O and CH_4-air-CO_2 are performed using COSILAB code and the GRI3.0 Mech as kinetic mechanism (Smith et al.). Note that the GRI-Mech 3.0 mechanism has been validated for CH_4-air-H_2O (Boushaki et al 2012, Mazas et al 2011) and CH_4-air-CO_2 (Wang et al. 2020) mixtures. The laminar burning velocity is an important parameter for validating chemical kinetics, modeling of turbulent combustion and the design of practical devices (Zachary et al. 2011). Figure 3 (left) shows the calculated laminar burning velocity with the equivalence ratio at 1 bar and 300K for CH_4-air, CH_4-air-10%H_2O and CH_4-air-10%CO_2 mixtures. The flame velocity is very sensitive to the dilution percent. For instance, a 10% of CO_2 results in a decrease of approximately 32% in the flame velocity (37.6 against 25.6 cm/s) for Φ=1. Figure 3 (right) clearly demonstrates the significant reduction of the laminar burning velocity with CO_2 and H_2O dilution. A dilution of 20% yields a reduction in S_L from 45 cm/s to 18 cm/s and 12 cm/s for H_2O and CO_2 addition, respectively, using oxygen-enriched CH_4 flame (25% of O_2). This is possibly due to thermal-diffusion effects of CO_2 dilution with decreasing adiabatic flame temperature.

12

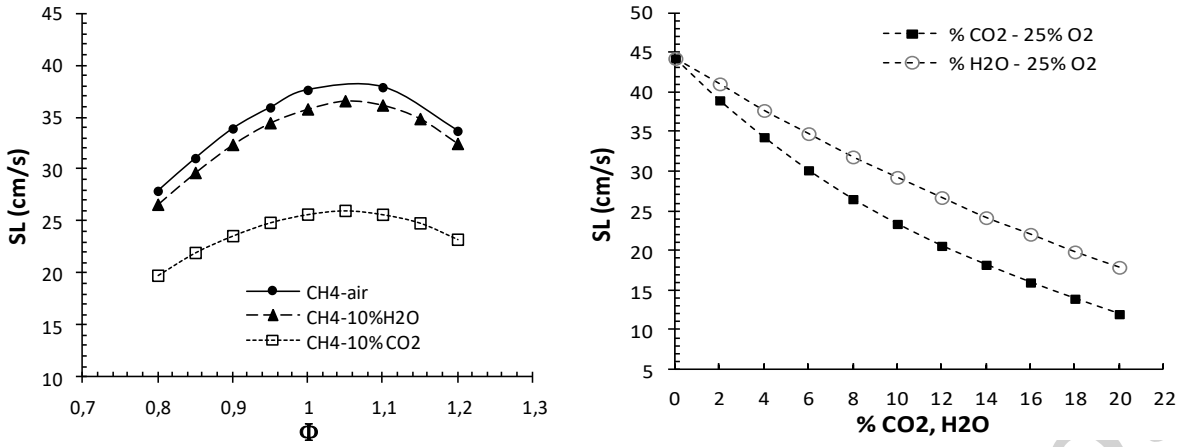

Fig. 3 (Left) Calculated laminar burning velocity (S_L) as a function of equivalence ratio (Φ) for different mixtures. (Right) S_L of CH_4-air as a function of H_2O and CO_2 dilutions for 25% of O_2, Φ=0.8, P=1 bar and T=300K

H_2O addition has significant chemical and thermal effects on the burning velocity as well, especially in lean and near-stoichiometric conditions, as also reported by Mazas et al. (2011). Chakroun et al. (2018) mentioned a chemical effect of CO_2, which has a bigger impact on the consumption speed and flame extinction strain rate than the effect of transport properties and Lewis number differences. They noted the important role of the extinction strain rate that highly impacted by the reaction $CO_2+H \Leftrightarrow CO+OH$. These results were also reported in (Glarborg and Bentzen 2008, Watanabe et al. 2013).

a)	b)	c)

13

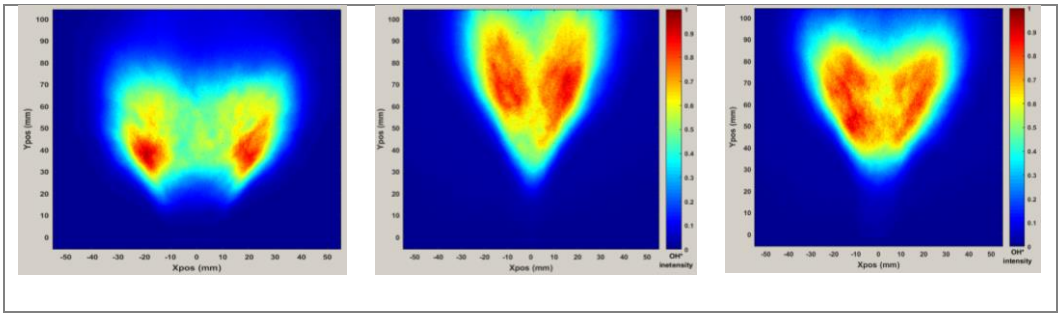

Fig. 4 OH* mean images of CH_4-air flames at Φ=0.8 and S_n=0.8, a) without dilution, b) 20% CO_2, c) 20% H_2O.

In the following sections, the experimental results on the turbulent swirling flame are presented and discussed. The impact of CO_2 and H_2O dilution on the instantaneous and averaged turbulent swirling flame fronts is examined. Figure 4 shows OH * mean values illustrating the effect CO_2 and H_2O dilution on the overall shape of flame. It is observed that the dilution with H_2O and CO_2 induces additional lifting of the flame base. The effect of CO_2 is relatively more pronounced than that of H_2O. With the CO_2 dilution, the flame base becomes thinner and shifts upwards away from the burner. At high dilution (16-20%), especially with CO_2, direct visualizations show non-negligible flame fluctuations at the stabilization zone. Beyond 20% CO_2 and 30% of H_2O the flame blows out. To help maintain the flame stability, the enrichment by oxygen is used.

Figure 5 presents the results of the liftoff heights (L_{OH}) without (21% O_2) and with oxygen enrichment (25% O_2). It is remarked that the O_2 enrichment decreases the liftoff height and enhances the flame stability (Fig. 5a-b). As observed above, the dilution by CO_2 (Fig. 5a) and H_2O (Fig. 5b) yields an increase of the lift-off height. For example, between 0 and 20% of dilution, L_{OH} increases from 20 to 38 mm (90% increase) and 33 mm (65% increase) with CO_2 and H_2O additions, respectively, for the case of 21%of O_2. This behavior may be related to the aforementioned flame speed results. Clearly, the dilution decreases the burning velocity and therefore the flame stabilizes at a further downstream. Furthermore, 25% O_2 enrichment (+4%

14

compared to air) enables the reduction of the liftoff height, to improve the flame stability and to operate with favorable conditions of stabilization. Another way to gain flame stability is to increase the swirl number, as observed in Fig. 5c. Here, remarkable drops in L_{OH} are captured with the increase of S_n. Without dilution, L_{OH} decreases from 16.5 mm to 8.5 mm as S_n increases from 0.8 to 1.4 (95% L_{OH} reduction). This is possibly due to enhanced flow rotational effect, which allows for the stabilization of the flame further upstream. Swirling flow improves the entrainment of gases and increases the stability limits of the flame. In summary, in the case of diluted combustion, the increase of swirl intensity, O_2 enrichment or the combination of both are effective means for improving flame stability. The flame length is also influenced by the dilution, the O_2 enrichment and the swirl intensity. Increasing swirl brings the IRZ (Internal Recirculation Zone) closer to the burner (and the average stagnation point) and the flame tends to stabilize around this zone (Beér and Chigier 1972, Zachary et al. 2011).

a)

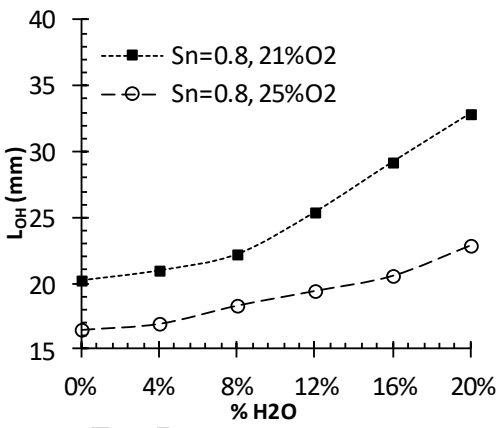

b)

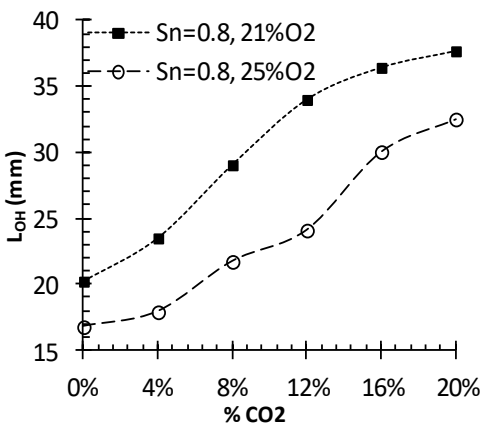

c)

15

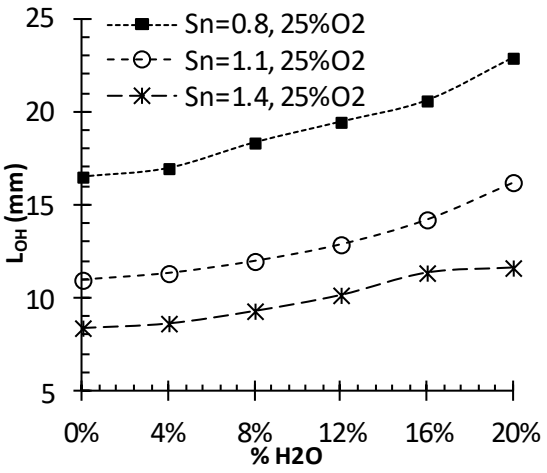

Fig. 5 Flame liftoff height (L_{OH}), (a) L_{OH} with CO_2 dilution, 21 and 25% O_2, S_n=0.8, (b), L_{OH} with H_2O dilution, 21 and 25% O_2, S_n=0.8, (c) L_{OH} with H_2O dilution and the swirl number (S_n=0.8, 1.1 and 1.4) at 25% O_2

Figure 6 presents the dependence of the flame length on the dilution percent, O_2 enrichment and swirl intensity. In industrial systems, the flame length is an important physical parameter since it defines the distance over which the heat flux can be captured. Here, the flame length is determined using OH* chemiluminescence by visualizing the top of the flame.

a)

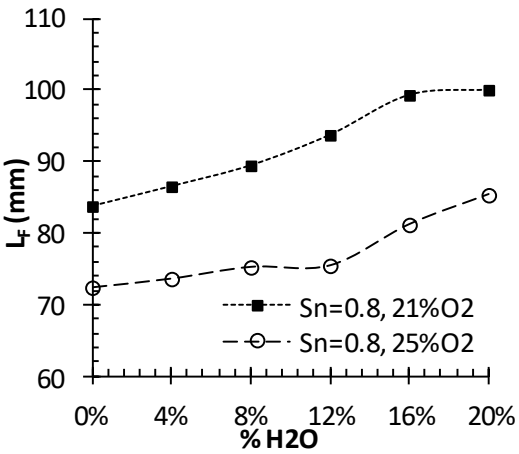

b)

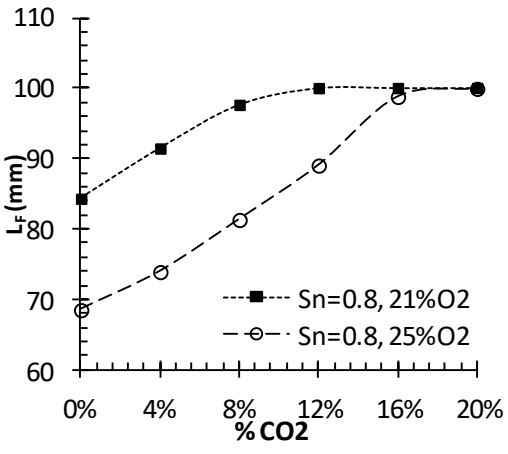

c)

16

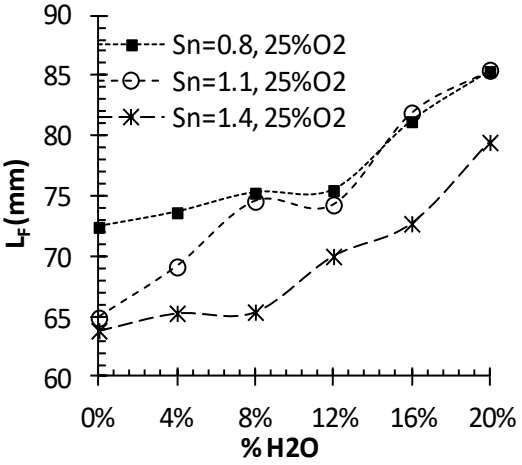

Fig. 6 Flame length (L_F), (a) L_F with CO_2 percent, 21 and 25% of O_2, S_n=0.8, (b), L_F with H_2O percent, 21 and 25% O_2, S_n=0.8, (c) L_F with H_2O dilution, 25% of O_2, S_n=0.8, 1.1 and 1.4.

The results show that the flame length (L_f) is influenced by dilution, oxygen enrichment and the swirl number. The flame length increases with higher CO_2-H_2O concentrations, as shown in Fig. 6 (a-b-c). Dilution changes the flame temperature and radical concentrations within the field, and lowers the burning velocity, whereas O_2 enrichment reduces the flame length (Fig. 6a-b). Further increase of the O_2 percent beyond 16% of CO_2 (Fig.6.b) dilution leaves insignificant variations in the corresponding flame lengths. It is noticed that L_F remains constant from 16% of CO_2 for 25% O_2 and from 12% of CO_2 for 21%O_2 (Fig. b). For air (21%O_2), higher CO_2 dilution disturbs the end of flame and fluctuations become higher, and the length in average seems remain constant. It is probably due to the same disturbance from a certain fraction of CO_2. Oxygen addition (Fig 6.a and b), however, increases the combustion temperature and the flame velocity, hereby allowing for a much rapid consumption of the underlying reactants. The flame becomes compact, intense, and more stable. The increase of swirl intensity decreases the flame length (Fig. 6c). With the increase of swirl intensity (Sn=1.4), the flame becomes wider and therefore shorter because of the flow's rotational effect. However, the effect of Sn (0.8 and 1.1) becomes very week from 8% of H_2O.

17

Pollutant emissions

Here, the evolutions of NOx and CO emissions as function of both CO_2 and H_2O contents are examined. The influence of oxygen enrichment and other parameters such as the global equivalence ratio and the swirl number have been investigated (Boushaki et al 2017, Chakchak et al 2022). Figure 7 shows the influence of CO_2 dilution on the flue gas temperature, NOx and CO emissions in the case of 25% O_2 enrichment. CO_2 dilution reduces the flue gas temperature (-100°C for 20% CO_2). This could be due to thermal effects associated with the high specific heat of CO_2, which reduces the overall heat release rate, besides the reduction of reactant concentrations in the mixture and chemical effects. This explains the reduction of NOx from 46 ppm to 2 ppm in the case of 20% dilution of CO_2, despite the O_2 enrichment. On the other hand, the CO concentration increases when CO_2 is added, due to the chemical effect of CO_2 as indicated in (Wang et al 2013).

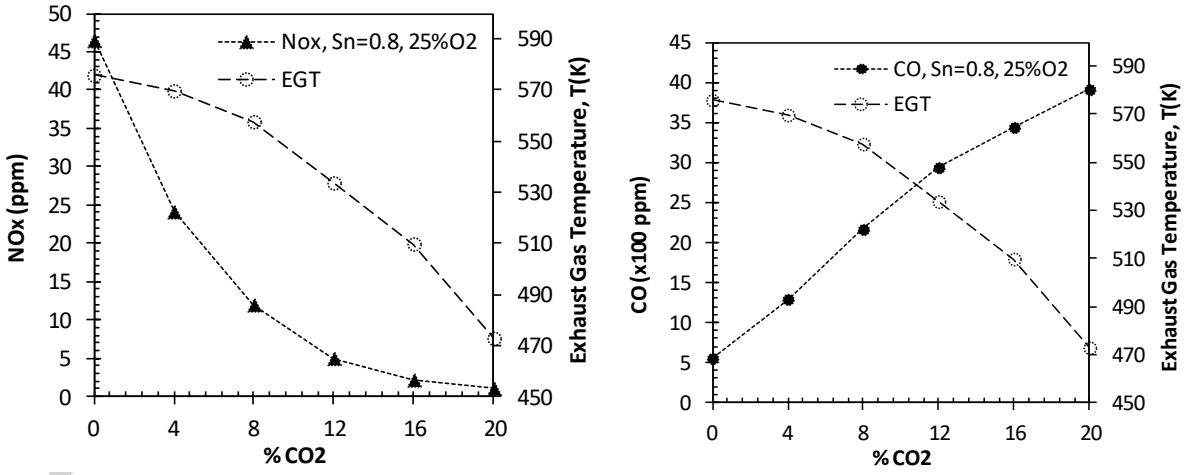

Fig. 7 NOx, CO emissions and Exhaust gas temperature with CO_2 dilution at 25%O_2, ϕ=0.8 and S_n=0.8

18

Figure 8 shows the results obtained by varying the amount of water vapor in the oxidizer from 0 to 20% (in vol.) for an equivalence ratio of 0.8 and a swirl number of 1.4. Like the case of CO_2 dilution, the temperature of the flue gases decreases significantly with the H_2O dilution following the drop in the flame temperature, which consequently limits the corresponding thermal NOx formation. It should be noted that CO concentration increases with the vapor water dilution because of temperature drop that quenches CO oxidation to CO_2 through CO+OH reactions. These results are so-far encouraging; the imposed dilution yields remarkable reduction in NOx emissions whereas the presence of O_2 promotes flame stability which can be impacted by dilution, nevertheless increasing CO remains challenging.

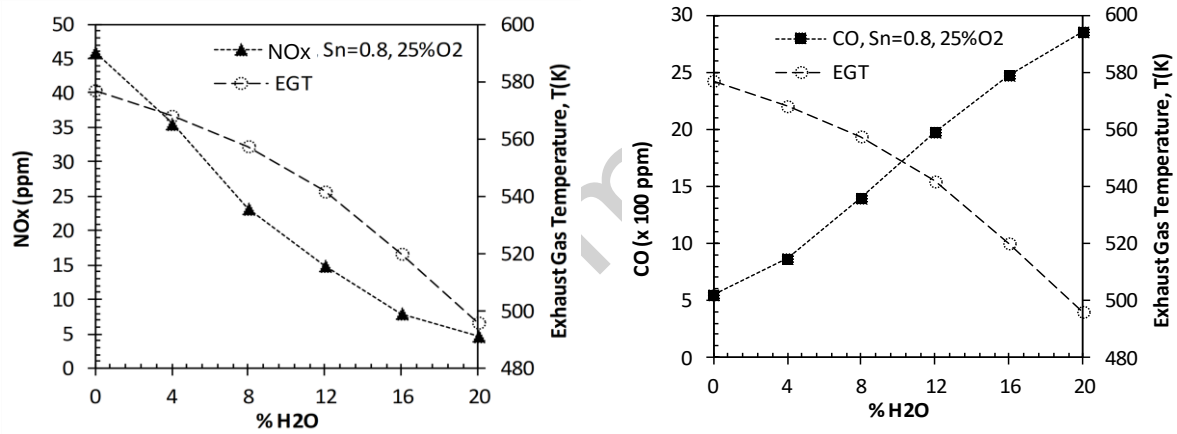

Fig. 8 NOx emissions, CO emissions and exhaust gas temperature with H_2O dilution at 25%O_2, ϕ=0.8 and S_n=0.8

Velocity fields

To further characterize the turbulent flow field along with its associated coherent vortical structures through the specification of the three velocity components of the swirl burner, Stereo Particle Image Velocimetry (Stereo-PIV) technique is employed for both non-reactive and reactive conditions. Figure 9 shows the mean field of the axial and the swirl velocity

19

components for the case of 0% dilution, Φ=0.8, S_n=0.8 and 21% O_2. The flame front is added (red lines denoted as flame base) to indicate the stabilization zone of flame. The axial velocity (V) field (Fig. 9a) clearly shows the central recirculation zone (CRZ), with negative velocity values (blue zone), surrounded by a second zone of high velocities corresponding to the annular part of the burner. This CRZ is induced by the swirl effect and accentuated by the presence of the central tube in the burner. This is the zone that offers a better flame stability, especially with the increase of the swirl intensity as shown in Fig. 5c. The position of the flame base is used to mark to mark the particular region within the flow field where the flame can be stabilized. This data obtained chemiluminescence on OH* as introduced in Figs. 4 and 5. The interesting information to extract from these results is that the flame stabilizes in areas of low longitudinal velocities; here, in the blue zone of the velocity fields (V falls between 0 and -1.5 m / s).

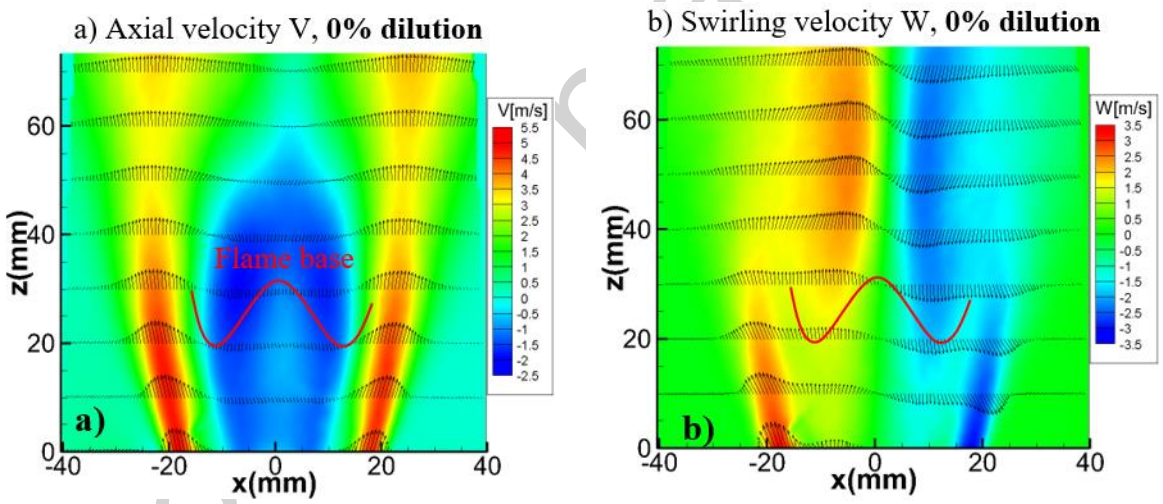

Fig. 9 a) Mean axial velocity (V) (with axial velocity in color scale and vectors determined by V and U). b) Mean swirling velocity (W) (with swirling velocity in color scale and vectors determined by W and U). Case: 0% dilution, Φ=0.8; S_n=0.8 and 21% of O_2. Red line represents the flame front at the stabilization point

20

Figure 9 (b) shows that the swirl velocity (W) is high since its value varies in the range of ±3 m/s. This was expected because of the helical flow induced by the swirler. Note that the vectors plotted in this figure are determined according to the measured swirling (W) and radial (U) velocity components. The negative value of W on the right side of the field is due to the swirling flow which goes in the opposite direction to that of the left side. It is observed that the swirling flow appears across the entire jet including the CRZ, which is accentuated with the presence of the flame compared to the non-reacting flow. It is worth noting that the base of flame is located in the zones with low swirling velocities as in the case of axial velocities.

Figure 10 illustrates the mean velocity fields with 16% of CO_2 dilution. Two important observations to report on the effect of CO_2 addition on the axial and swirling velocity fields. First, the extension of the CRZ (Fig. 10.a) and second, the restriction of the swirling flow domain to the central zone of the burner (Fig. 9.b). The effect of CO_2 dilution on the velocity fields may a priori contribute towards having a different flame shape and as previously discussed. Note that the influences of H_2O and CO_2 dilution on flow field of velocities are nearly similar, with more impact on the axial velocity for the latter.

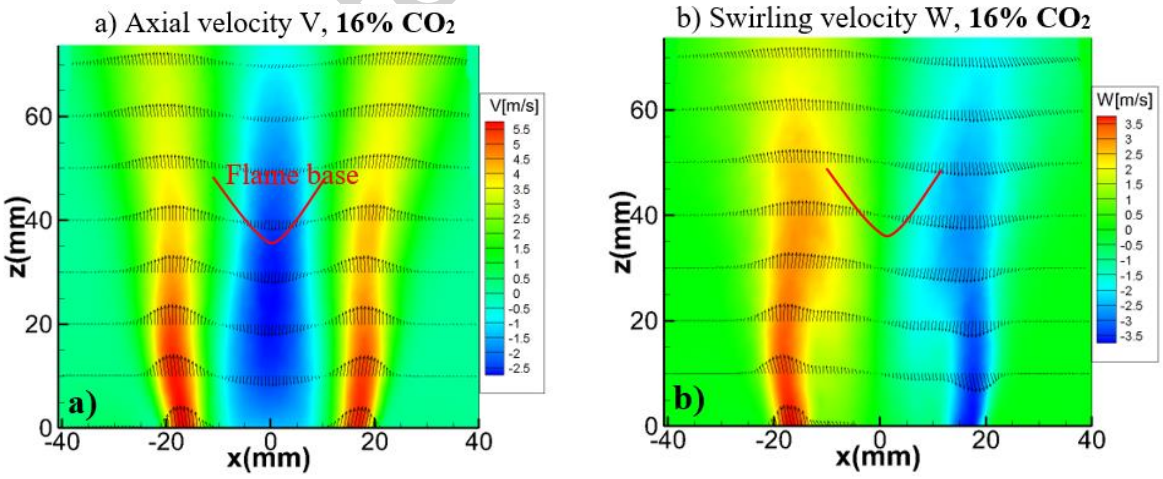

Fig. 10 Mean axial (a) and swirling (b) velocities with 16% CO_2 dilution (Φ=0.8, S_n=0.8 and 21% O_2). Red line refers to the flame front at the stabilization point

21

In Fig. 11, the effect of H_2O dilution on the axial and swirling velocities are shown for the case of 16% H_2O, Φ=0.8, S_n=0.8 and 21% of O_2. The influence of dilution is similar to the CO_2 case but with lesser amplitudes for the axial velocity, however, the penetration of the swirling flow toward the center of the burner is more pronounced with H_2O dilution. Likewise, the H_2O-diluted flame stabilizes in regions of low velocity ranges for both velocity components (V and W) as pointed out in (Fig. 11a-b).

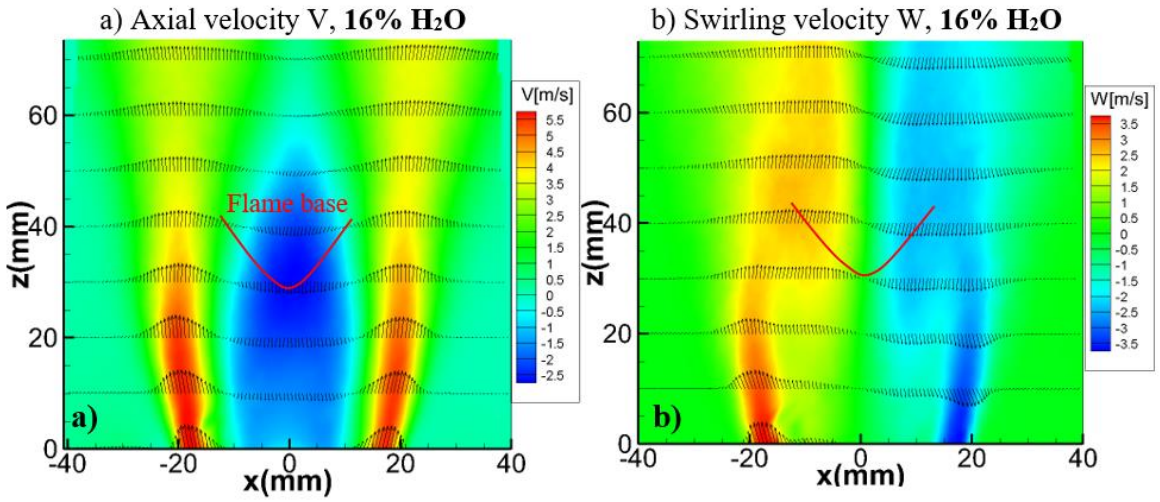

Fig. 11 a) Mean fields of axial velocity (V), b) Mean fields of swirling velocity (W). Case: with 16% of H_2O dilution, Φ=0.8, S_n=0.8 and 21% of O_2

Figure 12 compares the velocity profiles in the non-reactive and reactive cases both with and without dilution (0% dilution, 16% of CO_2, 16% of H_2O). Without dilution, the comparison indicates higher axial velocity (Fig. 12a) in the reactive case, because of the gas expansion caused by combustion. The maximum axial velocity is 3 m/s for the non-reacting flow while it is found to be around 4.2 m/s with flame. Flow acceleration is further observed in the central recirculation zone (CRZ), -2 m/s against -1 m/s for the reactive and non-reactive cases, respectively. In addition, higher radial expansion with a larger recirculation zone is observed in

22

the reacting flow. The topology of the swirling reacting flow velocity (Fig. 12b) is also impacted by the presence of flame, especially in its form. Dilution modifies slightly the corresponding velocity fields. Notice that the flow rate of the oxidizer is kept constant with or without dilution. In the case of CO_2/HO_2 dilution, the results reveal that the maximum velocity in the annular part is slightly higher and the flow is narrower. In the central recirculation zone, the velocity is also higher with dilution.

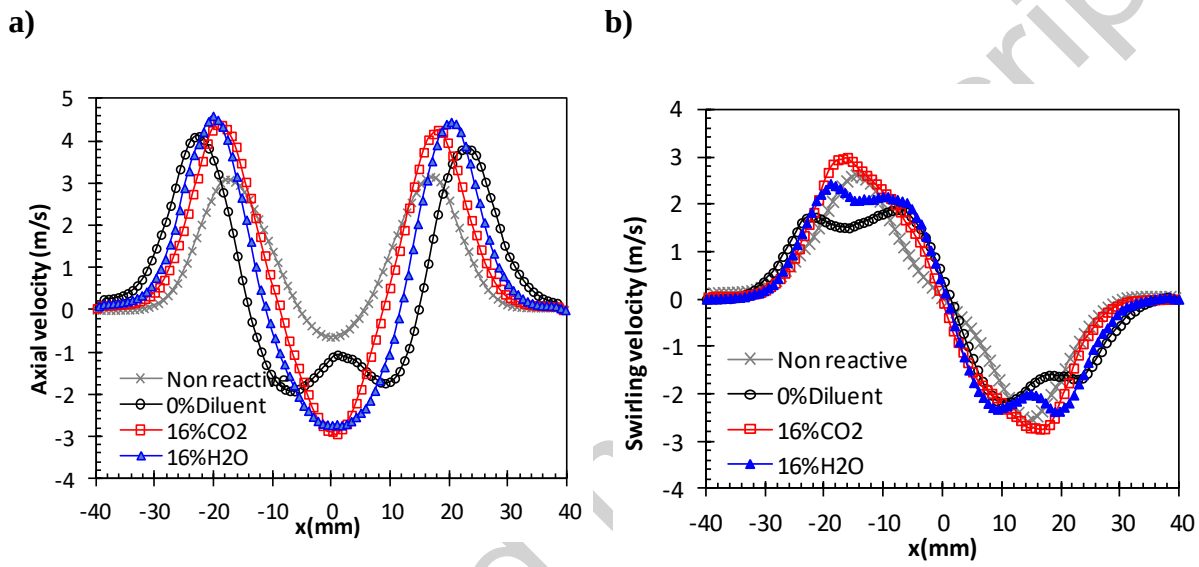

Fig. 12 Profiles velocities at Z=30mm without dilution and with 16% CO_2-H_2O dilution, a) axial velocity, b) swirl velocity (Sn=0.8, Φ=0.8 and 21% O_2)

Conclusions

The effects of oxygen enrichment and CO_2-H_2O dilution on non-premixed swirling turbulent flames were investigated. The burner has a coaxial configuration with a swirler in the annular part for the oxidizer and a central tube with radial injection for CH_4. The study included the flame shape and stability, the laminar burning velocity, the CO and NOx emissions and the flow fields as characterized by Stereo-PIV. The fraction of diluents varies from 0 to 20%, the

23

O_2 enrichment ranges from 21 to 25% (in vol.) and the swirl number varies from 0.8 to 1. The results can be summarized as follows:

1. The laminar burning velocity decreases markedly with dilution, and particularly with CO_2 addition because of its thermal-diffusion effects.
2. O_2 enrichment decreases the liftoff height and enhances the flame stability, however, dilution using CO_2 and H_2O causes an increase of the flame lift-off height due to the reduced flame speed. Two ways are suggested to compensate such effect and enhance flame stability: smaller fraction of O_2 enrichment (25%), and the increase of the swirl intensity.
3. The flame length increases with CO_2-H_2O addition possibly due to the delayed oxidation rates, however, the increase of swirl intensity or O_2 addition decreases the flame length.
4. Dilution also reduces drastically NOx emissions even for oxygen-enriched flame. For 20% of dilution and 25% of O_2 enrichment, NOx is strongly decreased to 4 and 2 ppm with H_2O and CO_2, respectively. Yet, CO emissions increase with CO_2 and H_2O dilutions.
5. Stereo-PIV measurements reveal the 3D structure of the swirled flow through the three velocity components. The mean vortical motion and the resulting central recirculation zone (CRZ) are clearly observed and analyzed. The CRZ due to the swirl improves flame stability, in particular with the increase of the swirl intensity. The results showed that the flame stabilizes in zones of low axial and swirling velocities.
6. In the case of CO_2/HO_2 dilution, the maximum velocity in the annular part and in the CRZ is slightly higher and the flow is narrower. Besides, with dilution, the extension of the CRZ and the decrease of swirling flow in the central zone of the burner were marked. Without dilution, the comparison between the reacting and non-reacting flow indicates the higher values of velocities, and the greater radial expansion of flow with a larger recirculation zone in the case of reacting flow.

24

Acknowledgements

Support from the Labex CAPRYSSES (ANR-11-LABX-006-01) is gratefully acknowledged. The authors would like to acknowledge the Reacting Gas Dynamics Lab in MIT, Cambridge USA, for their support.

Funding

Funding of the work from Labex CAPRYSSES (ANR-11-LABX-006-01), France.

Conflict of interest

The authors have no conflict of interest to declare that are relevant to the content of this article.

Ethical approval

This article does not contain any studies with human participants or animals.

Informed consent

Informed consent was obtained from all individual participants included in the study.

Author contributions

T. Boushaki: Wrote the main manuscript text. Conceptualization, Validation, Editing, Resources, Visualization, Supervision, Project administration, Funding acquisition H. Ziadaoui, S. Chakchak A. Ghabi: Investigation, prepared Figures, Formal analysis A.F. Ghoniem and A. Abd El-Rahman: Review & Editing, Formal analysis.

Data Availability Statement:

Data sharing not applicable – no new data generated

25

References

Abd-Alla G. Using exhaust gas recirculation in internal combustion engines: a review. Energy Convers Manag, 43:1027-42 (2002)

Baukal CE, Gebhart B. Heat transfer from oxygen-enhanced/ natural gas flames impinging normal to a plane surface. Exp Therm Fluid Sci, 16:247-59 (1998).

Baukal, Charles E. Oxygen-Enhanced Combustion, 2nd edition, CRC Press LLC (2013).

Beér J.M., Chigier N.A, Combustion Aerodynamics, Applied Sci, Publishers Ltd (1972).

Boushaki T., Dhué Y., Selle L., Ferret B., Poinsot T., Effects of hydrogen and steam addition on laminar burning velocity of methane-air premixed flame: Experimental and numerical analysis. Int. J. Hydrog. Energy., 37, 9412-9422 (2012).

Boushaki T., Merlo N., Chauveau C., Gökalp I., Study of pollutant emissions and dynamics of non-premixed turbulent oxygen enriched flames from a swirl burner, Proc. Comb. Inst. 36, 3959-3968 (2017).

Branco J, Coelho P.J., Costa M., Experimental and numerical investigation of turbulent diffusion flames in a laboratory combustor with a slot burner, Fuel 175,182–190 (2016).

Chakchak S., Zaidaoui H., Hidouri A, Godard G., Boushaki T., Oxygen enrichment effects on CH_4-air turbulent flow characteristics in a coaxial burner, Comb. Sci. Technol, (2022).

Chakchak S, Hidouri A, Ghabi A, Ghoniem AF, Boushaki T., Experimental investigation on the stability of turbulent swirling methane/air-O2 flames, Experimental Thermal and Fluid Science, Vol 141, 2023,110772.

Chakroun N.W. Michaels D. Shanbhogue S.J. and Ghoniem A.F., Response of Premixed Stoichiometric Oxy Flames to Strain: Role of Chemistry and Transport, JPP Volume 34, Number 4 (2018).

26

Docquier N, Candel S. Combustion control and sensors: a review. Prog Energy. Combust Sci, 28 :107–50 (2002).

Glarborg P., Bentzen L.L.B., Chemical effects of a high CO_2 concentration in oxy-fuel combustion of methane, Energy Fuels, 22 (2008), pp. 291-29

Granados DA, Chejne F, Mejía JM, G_omez CA, Berrío A, Jurado WJ. Effect of flue gas recirculation during oxy-fuel combustion in a rotary cement kiln. Energy, 64:615 (2014).

Gu X. Zan S.S. Ge G.B. Effect on flow field characteristics in methane–air non-premixed flame with steam addition. Experiments in Fluids, 41 pp 829–837 (2006).

Gupta AK, Lilley DG, Syred N. Swirl flows: Abacus Press, (1984).

Jangi M, Lucchini T, D'Errico G, Bai XS. Effects of EGR on the structure and emissions of diesel combustion. Proc Combust Inst, 34:3091-8 (2013).

Jeong Park, June Sung Park, Hyun Pyo Kim, Jeong Soo Kim, Sung Cho Kim, Jong Geun Choi, Han Chang Cho, Kil Won Cho, and Heung Soo Park, NO Emission behavior in Oxy-fuel combustion recirculated with carbon dioxide, Energy Fuels, 21, 121-129 (2007).

Le Cong T, Dagaut P, Oxidation of H_2/CO_2 mixtures and effect of hydrogen initial concentration on the combustion of CH_4 and CH_4/CO_2 mixtures: Experiments and modelling, Proc. Comb. Inst., vol 32, 1, P. 427-435 (2009).

Mansour M., Chen Y.G., Stability characteristics and flame structure of low swirl burner, Exp. Therm. Fluid Sci, Vol 32, Issue 7, Pages 1390-1395 (2008).

Mansouri Z., Boushaki T., Experimental and numerical investigation of turbulent isothermal and reacting flows in a non-premixed swirl burner, Int. J. Heat Fluid Flow, Vol. 72, Pages 200–213 (2018).

Mazas A.N., Fiorina B., Lacoste D.A., Schuller T. Effects of water vapor addition on the laminar burning velocity of oxygen enriched methane flames, Combust. Flame 158 (12) 2428-2440 (2011).

27

Merlo N., Boushaki T., Chauveau C., de Persis S., Pillier L., Sarh B., and Gökalp I.. Experimental Study of Oxygen Enrichment Effects on Turbulent Nonpremixed Swirling Flames. Energy Fuels, 27, 6191−6197 (2013).

Minamoto Y, Dunstan TD, Swaminathan N, Cant RS. DNS of EGR-type turbulent flame in MILD condition. Proc Combust Inst,34 :3231-8 (2013).

Poinsot T., Veynante D., Theoretical and numerical combustion, 2nd ed. Ed, RT (2009).

Qiu K, Hayden ACS. Increasing the efficiency of radiant burners by using polymer membranes. Appl Energy, 86:349-54 (2009).

Sher E. Handbook of air pollution from internal combustion engines: pollutant formation and control. Academic Press (1998).

Shimokuri D, Fukuba S, Ishizuka S. Fundamental investigation on the fuel-NOx emission of the oxy-fuel combustion with a tubular flame burner. Proc Comb Inst, 35:3573, (2015).

Smith Gregory P., Golden David M., Frenklach Michael, Moriarty Nigel W., Eiteneer Boris, Goldenberg Mikhail, Bowman C. Thomas, Hanson Ronald K., Song Soonho, Gardiner William C., Lissianski Jr. Vitali V., and Qin Zhiwei http://www.me.berkeley.edu/gri_mech

Taamallah S., Chakroun N.W., Watanabe H., Shanbhogue S.J, Ghoniem A.F., On the characteristic flow and flame times for scaling oxy and air flame stabilization modes in premixed swirl combustion, Proc. Comb. Inst., vol. 36, 3, Pages 3799-3807 (2017).

Wang L, Liu Z., Chen S., Zheng C., Li J., Physical and chemical effects of CO_2 and H_2O additives on counter flow diffusion flame, Energy Fuels 27, 7602–7611 (2013).

Wang S., Wang Z., He Y., Han X., Sun Z., Zhu Y., Costa, Laminar burning velocities of $CH_4/O_2/N_2$ and oxygen-enriched $CH_4/O_2/CO_2$ flames at elevated pressures measured using the heat flux method, Fuel 259, 116152 (2020).

28

Watanabe H., Arai F., Okazaki K., Role of CO_2 in the CH_4 oxidation and H_2 formation during fuel-rich combustion in O_2/CO_2 environments, Combust. Flame, 160 (2013).

Wu K.K., Chang YW, Chen C.H., Chen Y.D., High-efficiency combustion of natural gas with 21-30% oxygen enriched air, Fuel 89, 2455-2462 (2010).

Yu B, Kum SM, Lee CE, Lee S. Effects of exhaust gas recirculation on the thermal efficiency and combustion characteristics for premixed combustion system. Energy 2013; 49:375-83.

Yu B, Lee S, Lee CE, Study of NOx emission characteristics in CH_4/air non-premixed flames with exhaust gas recirculation; Energy, 91:119-127 (2015).

Yuasa S., Effects of swirl on the stability of jet diffusion flames, Combust. Flame 66 (181-192 (1986).

Zachary A. LaBry, Santosh J.Shanbhogue, Raymond L. Speth, Ahmed F. Ghoniem, Flow structures in a lean-premixed swirl-stabilized combustor with microjet air injection, Proc. Comb. Inst., Volume 33, Issue 1, 2011, Pages 1575-1581.

Zaidaoui H, Boushaki T, Sautet JC, Chauveau C, Sarh B, Gokalp I. Effects of CO_2 dilution and O_2 enrichment on non-premixed turbulent CH_4-air flames in a swirl burner, Comb. Sci Tech. 190. 5:784-802 (2017).

Zheng M, Reader GT, Hawley JG. Diesel engine exhaust gas recirculation. a review on advanced and novel concepts. Energy Convers Manag, 45:883-900 (2004).